

ARTICLE

Received 24 Nov 2015 | Accepted 27 May 2016 | Published 12 Jul 2016

DOI: 10.1038/ncomms12064

OPEN

Germline *MC1R* status influences somatic mutation burden in melanoma

Carla Daniela Robles-Espinoza^{1,2,*}, Nicola D. Roberts^{1,3,*}, Shuyang Chen^{4,*}, Finbarr P. Leacy^{5,6}, Ludmil B. Alexandrov³, Natapol Pornputtpong⁷, Ruth Halaban⁸, Michael Krauthammer^{7,9}, Rutao Cui⁴, D. Timothy Bishop^{10,**} & David J. Adams^{1,**}

The major genetic determinants of cutaneous melanoma risk in the general population are disruptive variants (*R* alleles) in the melanocortin 1 receptor (*MC1R*) gene. These alleles are also linked to red hair, freckling, and sun sensitivity, all of which are known melanoma phenotypic risk factors. Here we report that in melanomas and for somatic C>T mutations, a signature linked to sun exposure, the expected single-nucleotide variant count associated with the presence of an *R* allele is estimated to be 42% (95% CI, 15–76%) higher than that among persons without an *R* allele. This figure is comparable to the expected mutational burden associated with an additional 21 years of age. We also find significant and similar enrichment of non-C>T mutation classes supporting a role for additional mutagenic processes in melanoma development in individuals carrying *R* alleles.

¹Experimental Cancer Genetics, The Wellcome Trust Sanger Institute, Hinxton, Cambridgeshire CB10 1SA, UK. ²Laboratorio Internacional de Investigación sobre el Genoma Humano, Universidad Nacional Autónoma de México, Campus Juriquilla, Boulevard Juriquilla 3001, Santiago de Querétaro 76230, Mexico. ³The Cancer Genome Project, The Wellcome Trust Sanger Institute, Hinxton, Cambridgeshire CB10 1SA, UK. ⁴Department of Pharmacology and Experimental Therapeutics, Boston University School of Medicine, Boston, Massachusetts 02118, USA. ⁵MRC Biostatistics Unit, Cambridge Institute of Public Health, Cambridge Biomedical Campus, Cambridge CB2 0SR, UK. ⁶Division of Population Health Sciences, Royal College of Surgeons in Ireland, Lower Mercer Street, Dublin 2, Ireland. ⁷Department of Pathology, Yale University School of Medicine, New Haven, Connecticut 06519, USA. ⁸Department of Dermatology, Yale University School of Medicine, New Haven, Connecticut 06519, USA. ⁹Program in Computational Biology and Bioinformatics, Yale University School of Medicine, New Haven, Connecticut 06519, USA. ¹⁰Section of Epidemiology and Biostatistics, Leeds Institute of Cancer and Pathology, University of Leeds, Leeds, LS9 7TF, UK. * These authors contributed equally to this work. ** These authors jointly supervised the work. Correspondence and requests for materials should be addressed to D.J.A. (email: da1@sanger.ac.uk).

Melanocortin 1 receptor (MC1R) is a G protein-coupled receptor expressed on the surface of melanocytes that signals to downstream effectors, such as the microphthalmia-associated transcription factor, to regulate skin pigmentation and to control cell proliferation and apoptosis¹. Melanin is generated by melanocytes in two major forms, pheomelanin and eumelanin. Unlike eumelanin, which is dark brown or black in colour, pheomelanin is red/orange, and is associated with type I/II skin, freckles, red hair and an inability to tan². People with this phenotype are generally highly photosensitive, and prone to sunburn when exposed to ultraviolet (UV) light³.

Population sequencing studies have revealed a number of null or hypomorphic *MC1R* alleles, which are collectively referred to as *R* alleles and are strongly associated with the red hair and light skin phenotype^{4,5}. Other missense variants are referred to as *r* alleles and are less strongly associated with this hair colour and complexion^{4,6}. While *R/R* individuals are generally red heads, and persons with 0 or 1 *R* alleles are rarely red heads, pigmentation traits such as degree of tanning after repeated UV exposure³ and skin reflectance⁷ depend additively on the number of *R* alleles. In addition to regulating skin pigmentation, MC1R signalling has been reported to increase phosphorylation of DNA repair proteins, initiating the DNA damage repair process, and also to activate survival pathways^{8–11}. As such, polymorphisms in *MC1R* have been linked to increased melanocyte apoptosis and inefficient DNA repair¹². Collectively these factors link *MC1R* variants to increased melanoma risk^{6,13,14}. In animal model systems, null alleles of *Mc1r* (*Mc1r^{e/e}*) have been shown to co-operate with *Braf^{V600E}* to promote melanoma development via mechanisms including enhanced lipid peroxidation, a phenotype rescued on an albino mouse background owing to a lack of pheomelanin production¹⁵. This has led to the suggestion that loss of MC1R function, even in the absence of UV light, may be oncogenic. Despite these insights, it is still unclear whether *MC1R* germline variant alleles influence the genome-wide somatic mutation burden in melanoma.

In this study, we set out to establish the contribution of germline *MC1R* alleles to the somatic mutation landscape of sporadic melanoma. Mutations found in melanomas are predominantly C>T transitions due to the production of cyclobutane pyrimidine dimers (CPDs) in response to solar UV damage, but other mutational classes such as C>A transversions have also been observed^{16–20}. Indeed, hotspot mutations in key driver genes, such as *BRAF* and *KIT*, are almost exclusively acquired as non-C>T mutations¹⁷. Our results indicate that individuals with one or two germline *MC1R* *R* alleles have a significantly higher somatic mutational load than individuals with no *R* alleles. This finding has implications for our understanding of melanomagenesis, as well as the identification of individuals at higher risk of developing melanoma.

Results

Samples. We analysed somatic single-nucleotide variants (SNVs) from two independent melanoma cohorts: melanoma samples from The Cancer Genome Atlas (TCGA) skin cutaneous melanoma (SKCM) collection²¹, and a data set from the Yale Melanoma Genome Project²². We studied only cases with stated ethnicity ‘white’ and with a histopathological diagnosis of cutaneous melanoma (excluding acral and mucosal melanoma which are not thought to be UV related). The TCGA data set included 273 tumour/germline exome pairs (out of the total collection of 343 samples), which comprised 43 from primary tumours and 230 from metastases (all from different patients)

(Methods section, Supplementary Data 1 and 2). The Yale data set was composed of 132 tumour/germline exome pairs, all of which were from whites with a confirmed diagnosis of cutaneous melanoma (28 primaries, 104 metastases) (Supplementary Data 3).

Variant calling and definition of SNV sets. To define *MC1R* genotypes for each patient we analysed germline binary alignment/map (BAM) files to identify and classify all non-synonymous and nonsense variants as either *R*, *r* or wild-type alleles using the method shown in Supplementary Fig. 1, and which is described in the Methods section. Since *MC1R* disruptive variants segregate on separate haplotypes, we assumed persons with two *R* alleles to be homozygotes or compound heterozygotes. Sample numbers for each *MC1R* genotype are shown in Supplementary Fig. 2, with additional details found in Supplementary Data 2 and 3, and Supplementary Table 1. In the TCGA cohort, 23 (8%) individuals had two *R* alleles, 112 (41%) individuals had one *R* allele, and 138 (51%) individuals had genotypes that were 0/0, *r*/0 or *r*/*r* (zero *R* alleles). In the Yale data set, five (4%) individuals had two *R* alleles, 54 (41%) individuals had 1 *R* allele, and 73 (55%) individuals had 0 *R* alleles.

We downloaded somatic variant calls from the TCGA that had been previously generated by three pipelines; the Broad Institute MuTect pipeline (version 119)²³, the Baylor College of Medicine CARNAC pipeline (version 1.0), and the bambam pipeline from University of California at Santa Cruz (UCSC; version 1.4). To generate a stringent call set for downstream analysis, we selected these previously generated SNVs that were agreed on by two or three of these pipelines (Methods section, Supplementary Fig. 3). Somatic variants from the Yale data set were generated as described previously²². For our analysis we counted double and triple-nucleotide variants separately as SNVs. These calls accounted for an average of 4.9% of all somatic variants (range 0–18%).

Modelling somatic SNV burden against *R* allele presence. For each of the six basic SNV classes (C>A, C>G, C>T, T>A, T>C and T>G), we modelled the relationship between expected somatic SNV burden and the presence of *MC1R* *R* alleles using negative binomial regression (Methods section). For the TCGA cohort, additional predictor variables were included to control for age, sex, sample type (primary or metastasis), tissue collection centre, body area, Breslow thickness, Clark’s level and ulceration status (Methods section, Supplementary Data 2). Missing values in these predictor variables (~12% of the data) were multiply imputed (Methods section). The first three predictor variables were available for the Yale data set (Supplementary Data 3), with no missing information.

Figure 1a shows the distribution of the somatic SNV counts per tumour in the TCGA melanoma cohort broken down by *R* allele presence, and Supplementary Table 2 shows the results of the negative binomial regression adjusted for the above-mentioned eight clinical variables. Figure 1b and Supplementary Table 3 show the equivalent results for the Yale data set adjusted for the three available clinical variables. For all six mutation types in both data sets, there was evidence of an increased burden of somatic SNVs in persons carrying one or two *R* alleles. After Benjamini–Hochberg correction for testing for six mutation classes, statistically significant ($P < 0.05$) differences in expected SNV counts were observed in four of the six mutation classes in the TCGA data set (Table 1, Supplementary Table 2), and in five out of six in the Yale data set (Table 1, Supplementary Table 3). Statistically significant differences in expected SNV count were observed for all six mutation classes in the combined data set (all adjusted $P < 0.01$, Table 1, Supplementary Table 4), with this analysis being performed adjusting for the clinical variables common to both collections. For fixed values of the other

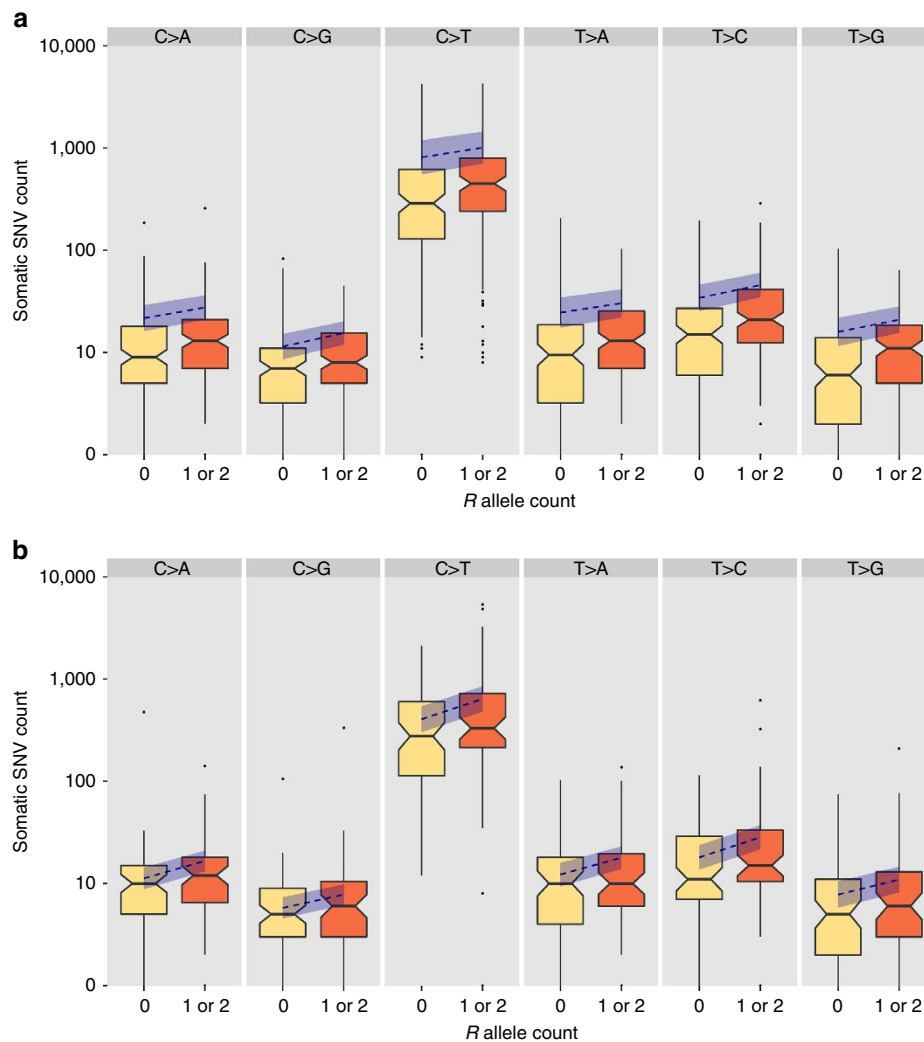


Figure 1 | The distribution of SNV counts detected through exome sequencing of melanoma samples. SNV counts are grouped by the presence of *R* alleles of the *MC1R* locus, and are shown as a boxplot with median, quartiles, whiskers and outliers. For each SNV class, the blue dashed line (and ribbon) charts the predicted mean mutation burden (and 95% confidence interval) of a patient with the most common constellation of values for clinical variables as the *R* allele count increases from zero to one or two, with all other clinical variables held fixed. **(a)** TCGA melanoma cohort, in which the most common constellation represents a 57-year-old male from the University of Sydney collection centre, with a metastasis to a regional lymph node of the extremities and a primary Breslow depth of 2.5 mm, Clark level IV, and no ulceration. Please note that one sample, TCGA-FW-A3R5, with *R* genotype 0/0 is an outlier with more than 10,000 C>T somatic mutations and is not depicted in the C>T panel of this image. **(b)** Yale Melanoma Project cohort, in which the most common constellation represents a 65 year-old male sampled via a metastasis.

predictors and for the C>T mutation class, carrying one or more *R* alleles was associated with a 24% (95% confidence interval (CI): –5 to 63%) increase in the expected somatic SNV count in the TCGA data set, a 58% (95% CI: 11–124%) increase in the Yale data set, and a 42% (95% CI: 15–76%) increase in the combined data set (Table 1, Supplementary Table 4). Aside from *MC1R* genotype, for the C>T mutation class in the combined data set, the other significant predictors of mutation burden were age (each extra year was associated with a 1.7% (95% CI: 0.9–2.4%) increase in the expected somatic SNV count) and tissue collection centre (Supplementary Table 4). Compared with the ‘baseline’ collection centre at the University of Sydney, melanomas from several other centres had significantly lower C>T mutational burdens, namely MD Anderson Medical Center, Greater Poland Cancer Centre, the University of Pittsburgh, Essen and Yale, whereas melanomas from The International Genomics Consortium had significantly higher numbers of this class of mutation (Supplementary Table 4). For the TCGA data set, a

location on the head and neck rather than the extremities and tissue collection centre were additional significant predictors of C>T somatic mutation burden (Supplementary Table 2). Results were similar for other mutation classes.

Alternative models for *R* allele presence and SNV count. We also considered alternative frameworks to model the relationship between *R* allele presence and somatic SNV count. Further analyses did not reveal any consistent patterns in expected mutation counts between individuals with one as compared with two *R* alleles (Methods section, Supplementary Fig. 4). A regression analysis in the combined data set considering the total number of SNV mutations instead of SNV mutation classes also found *MC1R* genotype to be a significant predictor of mutation count, along with age of diagnosis and tissue collection centre (Methods section, Supplementary Fig. 5), a result consistent with our other analyses.

Table 1 | Estimated multiplicative change in expected SNV count by *R* allele status adjusted for clinical and demographic variables.

Mutation class	TCGA					Yale					Combined					Extra years of age comparable to carrying <i>R</i> allele
	Multiplicative change expected SNV count in <i>R</i> carriers	Lower 95% CI	Upper 95% CI	<i>P</i> value	BH-adjusted <i>P</i> value	Multiplicative change expected SNV count in <i>R</i> carriers	Lower 95% CI	Upper 95% CI	<i>P</i> value	BH-adjusted <i>P</i> value	Multiplicative change expected SNV count in <i>R</i> carriers	Lower 95% CI	Upper 95% CI	<i>P</i> value	BH-adjusted <i>P</i> value	
C>A	1.28	1.04	1.57	0.01947	0.02921	1.48	1.11	1.98	0.00766	0.0212	1.4	1.18	1.66	0.0001	0.0002	23
C>G	1.36	1.11	1.66	0.00284	0.01359	1.35	1.02	1.79	0.03787	0.04544	1.27	1.07	1.52	0.00687	0.00687	29
C>T	1.24	0.95	1.63	0.11459	0.11459	1.58	1.11	2.24	0.0106	0.0212	1.42	1.15	1.76	0.00129	0.00194	21
T>A	1.26	1	1.59	0.05331	0.06397	1.46	1.07	2	0.0177	0.02655	1.32	1.09	1.61	0.00461	0.00553	18
T>C	1.34	1.1	1.64	0.00453	0.01359	1.57	1.13	2.18	0.00716	0.0212	1.6	1.33	1.92	0	0.00001	26
T>G	1.32	1.06	1.65	0.01197	0.02393	1.4	0.98	1.99	0.06226	0.06226	1.49	1.23	1.81	0.00005	0.00016	20

CI, confidence interval; SNV, single-nucleotide variant; TCGA, The Cancer Genome Atlas.

Adjusted incident rate ratios for *R* allele carriers compared to non-carriers together with 95% confidence intervals obtained via negative binomial regression. *P* values assess the null hypothesis that the incident rate ratio equals one, separately for the TCGA data set (adjusted for all available clinical data), the Yale data set (adjusted for all available clinical data) and the combined data set (adjusted for the clinical variables common to both datasets) with a Benjamini-Hochberg *P* value correcting for multiple testing of the six hypotheses (mutation classes) in the combined data set. The extra years of age with an effect size comparable to carrying an *R* allele is the ratio of the regression coefficient for *R* carrier status divided by the per year regression coefficient for age. Further details can be found in Supplementary Tables 2, 3 and 4.

Comparison of mutational signature differences. To further investigate the mutational differences between *R* allele carriers and non-carriers, we examined somatic mutational signatures in a trinucleotide context²⁴ (Methods section). Eight mutational signatures explained 97.5% of mutations in the combined TCGA and Yale melanoma data set (Supplementary Figs 6 and 7). The sample group with one or two *MC1R* *R* alleles had a significantly lower prevalence of the signature linked to age-associated 5-methylcytosine deamination, a result presumably explained in part by their younger age at diagnosis (57.6 versus 62.2 years on average; Supplementary Table 5). No other significant differences in the mutational signatures were identified^{24,25}.

Investigation of the role of *MC1R* in melanocyte biology. We next considered whether the increased number of mutations observed in tumours from *MC1R* variant carriers could be due to differential DNA repair ability in primary human melanocytes (HPMs). Therefore, we elected to explore the role of *MC1R* in HPM cultures in response to UV light (Methods section, Fig. 2). *MC1R* wild-type melanocytes were transfected with short hairpin RNA (shRNA) constructs resulting in the suppression of *MC1R* expression, or with a scrambled control shRNA, thus creating an isogenic pair of cell lines for functional studies. Importantly, knockdown of *MC1R* reduced but did not abolish *MC1R* expression, analogous to *MC1R* expression in *R* allele heterozygotes^{26,27} (Fig. 2a, Supplementary Fig. 8). Irradiation of cell lines with escalating doses of UV light (302 nm) resulted in significantly reduced survival of *MC1R* knockdown cells compared with cells transfected with a scrambled shRNA control (Fig. 2b), and reduced activity of the transcription-coupled/nucleotide excision repair pathway, as evidenced by reduced luciferase activity in the host cell reactivation assay²⁸ (Fig. 2c). Reduced *MC1R* expression was also associated with increased levels of CPDs (Fig. 2d) and 6–4 pyrimidine photoproducts (6–4PP, Fig. 2e), a result in keeping with genetic models using melanocytes from *R* allele carriers^{8,10}.

Discussion

Most mutations found in melanoma genomes are likely to be passengers, and are thus reflective of the UV exposure and other mutagenic processes operative over a patient's lifetime. Our regression analyses suggest that the estimated increase in expected SNV count associated with the presence of an *MC1R* *R* allele for the C>T mutation class is comparable to the estimated increase associated with an additional 21 years of age in the combined data set, with similar estimates across the other

mutation classes (range 18–29 years; Table 1). *R* allele presence is also a significant predictor of total SNV count (Supplementary Fig. 5). Interestingly, our analysis did not reveal any consistent patterns in mutation counts between individuals with one as compared with two *R* alleles (Methods section, Supplementary Fig. 4). This suggests that the majority of persons with one *R* allele, who do not have a red hair/sun sensitivity phenotype, may still be highly susceptible to the mutagenic effects of UV light. Of note, it has been suggested that red haired, sun-sensitive individuals are more likely to practice sun avoidance^{29,30}, a factor that confounds ready interpretation of the association between mutation count and number of *R* alleles.

Our study finds that melanomas from individuals carrying *MC1R* *R* variants associated with red hair and freckling have a significantly higher somatic mutational burden than melanomas from individuals with no *MC1R* *R* variants. Intriguingly, while C>T mutations were the most common mutational class observed across all *MC1R* genotypes, all mutation classes were significantly and similarly increased. This might reflect a form of 'collateral damage' resulting from a decreased ability of cells in patients with *R* alleles to protect themselves from UV damage, or indicate that other mutational processes are operative in melanocytes from these patients. When we compared the mutational signatures present in *MC1R* *R* allele carriers to those present in non-carriers (Supplementary Figs 6 and 7), we observed no significant differences between the two groups apart from the age-associated 5-methylcytosine deamination, a result explained in part by the marginally younger average age of *MC1R* *R* allele carriers. This suggests that the same mutational processes are operative in *R* allele carriers as in non-carriers, but that the relative frequency of mutational events may be what differs between these groups. However, studies with larger sample sizes should be performed to further investigate this relationship.

Notably, studies in mice have proposed a non-UV path to skin tumourigenesis via pheomelanin, which has been shown to induce oxidative stress and lipid peroxidation¹⁵. Previous studies have also investigated the role of *MC1R* in the DNA damage response in melanoma cell lines, or in primary mouse cells in culture^{31–33}. Since DNA repair may be different in these systems when compared to non-transformed human melanocytes, we elected to explore the role of *MC1R* in HPM cultures in response to UV light. These experiments show that, in this system, *MC1R* knockdown significantly impairs survival and DNA repair (Fig. 2a–c), and was also associated with increased levels of CPDs (Fig. 2d) and 6–4PPs (Fig. 2e). While CPDs and 6–4PP are primarily associated with C>T and CC>TT mutations, they have also been associated with non-C>T mutations¹⁹, and thus

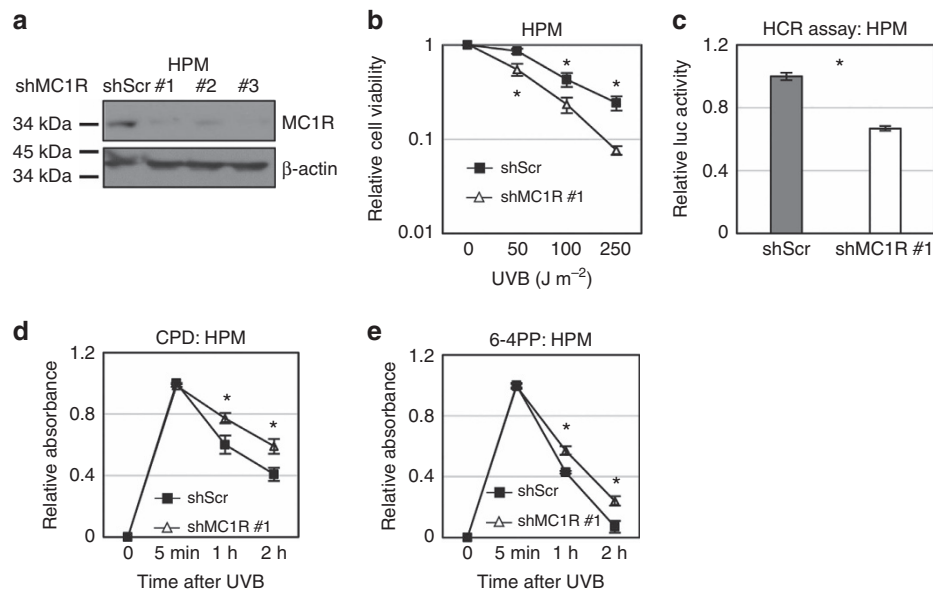


Figure 2 | *MC1R* expression regulates the formation of mutagenic photoproducts. (a) Shown are HPMs stably expressing control shRNA (shScr) or multiple independent shMC1Rs targeting *MC1R* (#1, #2, #3). Cells were pre-incubated with $1 \mu M$ α -MSH for 30 min, then exposed to $100 J m^{-2}$ UVB light, and harvested 3 h later for Western blot analysis. (b) HPM cells stably expressing shMC1R#1 were irradiated with different doses of UVB light as indicated. Cells were collected at 24 h after UVB light irradiation and viability assessed using the 3-(4,5-dimethylthiazol-2-yl)-2,5-diphenyltetrazolium bromide (MTT) assay. (c) HPMs stably expressing an shRNA against *MC1R* (shMC1R#1) or a scrambled control (ShScr) were transfected with $2 \mu g$ of UV damaged pGL3 luciferase expression vector and $0.5 \mu g$ pRL Renilla Luciferase control reporter vector before the host cell reactivation assay^{28,32} (Methods section; d,e). HPMs stably expressing an shRNA against *MC1R* (shMC1R#1) or a scrambled control (ShScr) were irradiated with $100 J m^{-2}$ UVB light and then collected at the different time points indicated. Genomic DNA was extracted and photoproducts were detected by ELISA. Cyclobutane pyrimidine dimer (CPD) (d) or 6-4 pyrimidine photoproduct (6-4PP) (e) antibodies were used (Methods section). These data were compiled from three separate experiments performed in triplicate. Significance ($*P < 0.05$) was calculated by using the unpaired two-tailed Student's *t*-test comparing the means (shScr vs shMC1R#1) of the three experiments. Error bars represent s.d.

may contribute to the elevated levels of these mutations observed in *R* allele carriers. Importantly, a recent study has shown that sequence context markedly affects the mutagenic effects of 6-4PP, and the resulting nucleotide change³⁴. Notably, N>T mutations have been observed¹⁹, and this may provide a mechanistic explanation for the enrichment of these mutations observed in our study. Thus, the enrichment of the non-C>T signatures we observe are likely to be the result of multiple mutagenic processes such as lipid peroxidation and ROS activity¹⁵, together with the effects of ultraviolet photoproducts such as 6-4PP.

In summary, we find a role for germline *MC1R* variants in influencing the somatic mutational landscape of melanoma. Since red heads comprise around 1–2% of the world's population, yet 16% of melanoma patients³⁵, and 26–40% of melanoma patients are *R* allele carriers³⁶, this work has significant implications for understanding the genesis of melanoma in these high-risk groups.

Methods

Clinical variables in TCGA cohort. For the TCGA melanoma cohort²¹, the available clinical variables included age at diagnosis, gender, tissue collection centre, body area, tissue type, Breslow depth, Clark level and ulceration status (Supplementary Data 2). The median age was 57 years (interquartile range 46–70, missing information for one sample), and the cohort included 99 females and 174 males. 112 samples were from the extremities, 106 from the trunk, 21 from the head and neck, 4 recorded as 'other' and 30 were unknown. 154 samples were from a regional lymph node, 45 from regional tissue, 43 from a primary tumour and 31 from a distant metastasis. 35 samples had Clark level V, 92 level IV, 51 level III, 13 level II, five level I and 77 with unknown Clark level. 85 samples were ulcerated, 98 had no ulceration and 90 were unknown. The median Breslow depth was 2.5 mm (interquartile range 1.2–5.0, unknown for 66 samples). Tissue collection centres were: The University of Sydney (EE) which contributed 86 samples, MD Anderson (D3) 55, Essen (FS) 36, the University of Pittsburgh (ER) 30, Asterand (EB) 27, the Greater Poland Cancer Center (D9) 11, Roswell (GN) 11, the University of North

Carolina (FR) 6, The International Genomics Consortium (FW) 5, ABS - IUPUI (GF) 3, Cureline (BF) 2 and The University of Miami (IH) 1.

Germline *MC1R* variant identification. Common *MC1R* variants have previously established classifications^{26,37,38}. To identify the precise variants carried by each individual, for each normal/germline BAM, we called variants in the *MC1R* region with samtools mpileup -Dsu -C50 -m2 -F0.0005 -d1000 and bcftools view -p 0.99 -vcgN, applying the standard set of vcf-annotate filters, and applying the Ensembl Variant Effect Predictor³⁹ to the canonical *MC1R* transcript (ENST00000555147) including SIFT⁴⁰ and PolyPhen⁴¹ scores. For each normal BAM, we extracted *MC1R* polymorphisms that passed all filters, including the nine canonical *MC1R* missense polymorphisms, nonsense or frameshift mutations and variants predicted to be deleterious or damaging by SIFT or PolyPhen (details below).

To classify rare alleles of *MC1R* as *R* or *r*, we used the SIFT 4.0.5 and PolyPhen 2.2.2 algorithms as indicated in Supplementary Fig. 1. *R* genotypes for each sample are provided in Supplementary Data 2 (TCGA) and Supplementary Data 3 (Yale). Of note, a recent report⁴² quantified membrane expression levels and cAMP induction by the rare *MC1R* alleles p.Gly89Arg, p.Thr95Met, p.Asp121Glu and p.Arg213Trp, found in patients from the TCGA cohort, as well as p.Ser83Leu, in the same position as a variant found in a patient from the Yale cohort (p.Ser83Pro). This study suggested that, whereas variants p.Gly89Arg, p.Asp121Glu and p.Ser83Leu were classified correctly by SIFT and PolyPhen 2 (all as *R* alleles), p.T95M might be more accurately classified as *r* and p.Arg213Trp as *R*. We have replicated the analysis described in this paper (using the methods described below) classifying p.Thr95Met as *r* and p.Arg213Trp as *R*. The results revealed that *R* allele count was still a significant predictor of the overall SNV mutation count. Coefficient estimates, 95% CIs, and *P* values for the *R* allele count predictor for each mutation class for this analysis are provided in Supplementary Table 6.

Identification of somatic variants calls. We downloaded VCF files containing somatic variant calls from CGHub⁴³. These calls were produced by the three TCGA analysis centres: the Broad Institute, Baylor College of Medicine, and UCSC. Variants marked as 'PASS' and called by at least two centres were included in subsequent analyses. We compared this set of calls with those released by the main analysis of the TCGA SKCM Working Group²¹ (Supplementary Fig. 3) revealing

high concordance. TCGA SKCM somatic calls were downloaded on August 2015 from http://tcga-data.nci.nih.gov/docs/publications/skcm_2015/.

Modelling the effect of R alleles on somatic mutation count. For each of the six basic SNV classes (C>A, C>G, C>T, T>A, T>C and T>G), we modelled the relationship between expected somatic SNV burden and the presence of MC1R R alleles using negative binomial regression with a log link (that is, modelling $\log(\text{expected SNV count})$). We controlled for all available clinical variables. Missing clinical variable values in the TCGA data set were imputed 10 times using the MICE package in R^{44,45}, with the variables age, Breslow thickness, gender, Clark level, ulceration, tissue source, tissue type, body area, R allele presence and the counts for each of the six basic mutational classes being included in the univariate imputation models⁴⁴. Values for any level of a categorical variable with <5 samples were also set to missing and imputed. For the Yale Melanoma data set, there were fewer clinical variables available but there was no missing information.

For our primary analysis, the estimates of the effect of carrying at least one R allele were compared with persons carrying zero R alleles.

Alternative models for R allele presence and SNV count. As described above, we compared the somatic mutation burden of melanomas from individuals with one or two R alleles to individuals with zero R alleles. We also considered an alternative model in which the somatic mutation count in the combined data set is regressed on R allele count (three levels) instead of presence/absence of an R allele (two levels; Supplementary Fig. 4). In this framework, the average increase in the expected C>T somatic SNV count associated with the presence of each R allele is comparable to the increased mutational burden associated with an additional 16.15 years of age. However, the numbers of R/R individuals in these cohorts is not sufficient to assess the contribution of R alleles individually.

We also considered a model in which total somatic SNV count in the combined data set is regressed on the presence or the absence of R alleles, instead of considering each mutation class separately (Supplementary Figure 5). This analysis is dominated by C>T mutations as they are much more abundant than the other mutational classes. The significant predictors of total somatic SNV count in this analysis were age at diagnosis, R allele presence and tissue collection centre.

Extraction of mutational signatures. We extracted mutational signatures in the trinucleotide context²⁴ *de novo* on the combined TCGA and Yale data sets using a Hierarchical Dirichlet Process⁴⁶ (HDP) with one child-DP node per sample, one parent-DP node per R allele group (zero or at least one R allele), and one grandparent-DP node with a uniform Dirichlet prior distribution. We initialized the HDP with four clusters, then ran four independent Markov chain Monte Carlo (MCMC) chains with 10,000 burn-in iterations and 500 posterior samples collected off each chain with 50 iterations between each (2,000 posterior samples in total). We performed all analyses with the 'hdp' R package version 0.1.0, available at github.com/nicolaroberts/hdp.

Melanocyte cultures and ultraviolet exposure. HPMs were isolated from foreskins as described previously⁴⁷ and cultured in Medium 254 from Life Technologies (Thermo Fisher Scientific, Waltham, MA) supplemented with 10% fetal bovine serum. Cells were washed with PBS twice and exposed to UVB light in a Stratelinker ultraviolet chamber (Stratagene, Cedar Creek, TX) fitted with ultraviolet B bulbs (UVP Inc. CA). Ultraviolet emittance was measured using an ultraviolet photometer (UV Products, Upland, CA, USA). An ultraviolet B dose of 100 J m⁻² is equivalent to one standard erythema dose of UVB light.

Plasmids and shRNA constructs. shRNA constructs targeting human MC1R (Cat. No. RHS4533-EG4157) were purchased from Open Biosystems (Thermo Fisher Scientific). The target sequence for shMC1R#1 is 5'-AAATGTCTCTTTA GGAGCCTG-3'.

Antibodies and western blot. Anti-MC1R (N-19; at a dilution of 1:500) antibody and Peroxidase-conjugated anti-goat secondary antibody (at dilution 1:2,000) were purchased from Santa Cruz Biotechnology, Inc. (Dallas, TX). Peroxidase-conjugated β -actin (ACTB, at dilution 1:10,000) antibody was purchased from Sigma-Aldrich (St. Louis, MO). Western blot analysis was performed as described previously⁴⁷.

DNA damage repair assays. CPD and 6-4PP ELISA were performed by using anti-CPD and anti-6-4PP antibodies, the purified anti-mouse IgG mAb was diluted to 2 $\mu\text{g ml}^{-1}$ in PBS and added into an enhanced protein-binding ELISA plate (for example, Falcon Labware plate). Antibodies specific for CPD (MC-062) and 6-4PP (KTM-50) were diluted 1:1,000 in blocking buffer and added to each well. Optical density at 405 nm was measured. For the host cell reactivation assay²⁸, pGL3 (Promega, Madison, WI) was irradiated at a dose of 700 J m⁻² of UVC light to induce DNA damage in the form of CPD and 6-4PP, which block transcription until repaired. Damaged pGL3 was transfected into cells using lipofectamine 2000 (Thermo Fisher Scientific). A *Renilla* vector was used as a transfection control.

Data availability. Data referenced in this study are available from TCGA melanoma data set: <https://cghub.ucsc.edu/>, filter by disease = SKCM, analyte type = DNA, study = TCGA, sample type = Blood derived normal (for germline DNA) or Metastatic (06), Primary solid tumour (01) for tumour samples, platform = Illumina, state = live, library type = WGS, WXS. Centre = BI was selected for germline DNA analysis. The Yale data set is available from dbGAP under accession code phs000933. The authors declare that all other data supporting the findings of this study are available within the article and its Supplementary Information files or available from the authors on request. Signature analyses were performed with the 'hdp' R package version 0.1.0, available at github.com/nicolaroberts/hdp. All scripts used to perform the analysis in this study is released as Supplementary Software 1.

References

- García-Borrón, J. C., Abdel-Malek, Z. & Jiménez-Cervantes, C. MC1R, the cAMP pathway, and the response to solar UV: extending the horizon beyond pigmentation. *Pigment Cell Melanoma Res.* **27**, 699–720 (2014).
- Nasti, T. H. & Timares, L. MC1R, eumelanin and pheomelanin: their role in determining the susceptibility to skin cancer. *Photochem. Photobiol.* **91**, 188–200 (2015).
- Healy, E. *et al.* Melanocortin-1-receptor gene and sun sensitivity in individuals without red hair. *Lancet* **355**, 1072–1073 (2000).
- Valverde, P., Healy, E., Jackson, I., Rees, J. L. & Thody, A. J. Variants of the melanocyte-stimulating hormone receptor gene are associated with red hair and fair skin in humans. *Nat. Genet.* **11**, 328–330 (1995).
- Beaumont, K. A., Shekar, S. N., Cook, A. L., Duffy, D. L. & Sturm, R. A. Red hair is the null phenotype of MC1R. *Hum. Mutat.* **29**, E88–E94 (2008).
- Raimondi, S. *et al.* MC1R variants, melanoma and red hair color phenotype: a meta-analysis. *Int. J. Cancer* **122**, 2753–2760 (2008).
- Sturm, R. A. *et al.* The role of melanocortin-1 receptor polymorphism in skin cancer risk phenotypes. *Pigment Cell Res.* **16**, 266–272 (2003).
- Cassidy, P. B., Abdel-Malek, Z. A. & Leachman, S. A. Beyond red hair and sunburns: uncovering the molecular mechanisms of MC1R signaling and repair of UV-induced DNA damage. *J. Invest. Dermatol.* **135**, 2918–2921 (2015).
- Jarrett, S. G., Wolf Horrell, E. M., Boulanger, M. C. & D'Orazio, J. A. Defining the contribution of MC1R physiological ligands to ATR phosphorylation at Ser435, a predictor of DNA repair in melanocytes. *J. Invest. Dermatol.* **135**, 3086–3095 (2015).
- Abdel-Malek, Z. A. *et al.* Melanocortins and the melanocortin 1 receptor, moving translationally towards melanoma prevention. *Arch. Biochem. Biophys.* **563**, 4–12 (2014).
- Swope, V. *et al.* Significance of the melanocortin 1 receptor in the DNA damage response of human melanocytes to ultraviolet radiation. *Pigment Cell Melanoma Res.* **27**, 601–610 (2014).
- Denat, L., Kadekaro, A. L., Marrot, L., Leachman, S. A. & Abdel-Malek, Z. A. Melanocytes as instigators and victims of oxidative stress. *J. Invest. Dermatol.* **134**, 1512–1518 (2014).
- Bishop, D. T. *et al.* Genome-wide association study identifies three loci associated with melanoma risk. *Nat. Genet.* **41**, 920–925 (2009).
- Pasquali, E. *et al.* MC1R variants increased the risk of sporadic cutaneous melanoma in darker-pigmented Caucasians: A pooled-analysis from the M-SKIP project. *Int. J. Cancer* **136**, 618–631 (2015).
- Mitra, D. *et al.* An ultraviolet-radiation-independent pathway to melanoma carcinogenesis in the red hair/fair skin background. *Nature* **491**, 449–453 (2012).
- Krauthammer, M. *et al.* Exome sequencing identifies recurrent somatic RAC1 mutations in melanoma. *Nat. Genet.* **44**, 1006–1014 (2012).
- Hodis, E. *et al.* A landscape of driver mutations in melanoma. *Cell* **150**, 251–263 (2012).
- Berger, M. F. *et al.* Melanoma genome sequencing reveals frequent PREX2 mutations. *Nature* **485**, 502–506 (2012).
- Ikehata, H., Ono, T., Tanaka, K. & Todo, T. A model for triplet mutation formation based on error-prone translesional DNA synthesis opposite UV photolesions. *DNA Repair (Amst)* **6**, 658–668 (2007).
- Pleasant, E. D. *et al.* A comprehensive catalogue of somatic mutations from a human cancer genome. *Nature* **463**, 191–196 (2010).
- Cancer Genome Atlas Network. Genomic classification of cutaneous melanoma. *Cell* **161**, 1681–1696 (2015).
- Krauthammer, M. *et al.* Exome sequencing identifies recurrent mutations in NF1 and RASopathy genes in sun-exposed melanomas. *Nat. Genet.* **47**, 996–1002 (2015).
- Cibulskis, K. *et al.* Sensitive detection of somatic point mutations in impure and heterogeneous cancer samples. *Nat. Biotechnol.* **31**, 213–219 (2013).
- Alexandrov, L. B. *et al.* Signatures of mutational processes in human cancer. *Nature* **500**, 415–421 (2013).
- Forbes, S. A. *et al.* COSMIC: exploring the world's knowledge of somatic mutations in human cancer. *Nucleic Acids Res.* **43**, D805–D811 (2015).

26. Beaumont, K. A. *et al.* Receptor function, dominant negative activity and phenotype correlations for MC1R variant alleles. *Hum. Mol. Genet.* **16**, 2249–2260 (2007).
27. Más, J. S., Gerritsen, I., Hahmann, C., Jiménez-Cervantes, C. & García-Borrón, J. C. Rate limiting factors in melanocortin 1 receptor signalling through the cAMP pathway. *Pigment Cell Res* **16**, 540–547 (2003).
28. Latimer, J. J. Analysis of actively transcribed DNA repair using a transfection-based system. *Methods Mol. Biol.* **1105**, 533–550 (2014).
29. Newton-Bishop, J. A. *et al.* Relationship between sun exposure and melanoma risk for tumours in different body sites in a large case-control study in a temperate climate. *Eur. J. Cancer* **47**, 732–741 (2011).
30. Dwyer, T. *et al.* Melanocortin 1 receptor genotype, past environmental sun exposure, and risk of multiple sclerosis. *Neurology* **71**, 583–589 (2008).
31. Jarrett, S. G. *et al.* PKA-mediated phosphorylation of ATR promotes recruitment of XPA to UV-induced DNA damage. *Mol. Cell* **54**, 999–1011 (2014).
32. Jagirdar, K. *et al.* The NR4A2 nuclear receptor is recruited to novel nuclear foci in response to UV irradiation and participates in nucleotide excision repair. *PLoS ONE* **8**, e78075 (2013).
33. Hauser, J. E. *et al.* Melanin content and MC1R function independently affect UVR-induced DNA damage in cultured human melanocytes. *Pigment Cell Res.* **19**, 303–314 (2006).
34. Shriber, P., Leitner-Dagan, Y., Geacintov, N., Paz-Elizur, T. & Livneh, Z. DNA sequence context greatly affects the accuracy of bypass across an ultraviolet light 6-4 photoproduct in mammalian cells. *Mutat. Res.* **780**, 71–76 (2015).
35. Olsen, C. M., Carroll, H. J. & Whiteman, D. C. Estimating the attributable fraction for melanoma: a meta-analysis of pigimentary characteristics and freckling. *Int. J. Cancer* **127**, 2430–2445 (2010).
36. Williams, P. F., Olsen, C. M., Hayward, N. K. & Whiteman, D. C. Melanocortin 1 receptor and risk of cutaneous melanoma: a meta-analysis and estimates of population burden. *Int. J. Cancer* **129**, 1730–1740 (2011).
37. Duffy, D. L. *et al.* Interactive effects of MC1R and OCA2 on melanoma risk phenotypes. *Hum. Mol. Genet* **13**, 447–461 (2004).
38. Davies, J. R. *et al.* Inherited variants in the MC1R gene and survival from cutaneous melanoma: a BioGenoMEL study. *Pigment Cell Melanoma Res.* **25**, 384–394 (2012).
39. Yates, A. *et al.* Ensembl 2016. *Nucleic Acids Res.* **44**, D710–D716 (2016).
40. Ng, P. C. & Henikoff, S. SIFT: predicting amino acid changes that affect protein function. *Nucleic Acids Res.* **31**, 3812–3814 (2003).
41. Adzhubei, I., Jordan, D. M. & Sunyaev, S. R. Predicting functional effect of human missense mutations using PolyPhen-2. *Curr. Protoc. Hum. Genet.* **Ch. 7**, Unit7.20 (2013).
42. Ozola, A. *et al.* Melanoma risk associated with MC1R gene variants in Latvia and the functional analysis of rare variants. *Cancer Genet.* **206**, 81–91 (2013).
43. Wilks, C. *et al.* The Cancer Genomics Hub (CGHub): overcoming cancer through the power of torrential data. *Database (Oxford)* **2014**, pii: bau093 (2014).
44. Zhang, Z. Multiple imputation with multivariate imputation by chained equation (MICE) package. *Ann. Transl. Med.* **4**, 30 (2016).
45. van Buuren, S. & Groothuis-Oudshoorn, K. mice: Multivariate Imputation by Chained Equations in R. *J. Stat. Softw.* **45**, 1–67 (2011).
46. Teh, Y. W., Jordan, M. I., Beal, M. J. & Blei, D. M. Hierarchical Dirichlet Processes. *J. Am. Stat. Assoc.* **101**, 1566–1581 (2006).
47. Cao, J. *et al.* MC1R is a potent regulator of PTEN after UV exposure in melanocytes. *Mol. Cell* **51**, 409–422 (2013).

Acknowledgements

This work was funded by Cancer Research UK and the Wellcome Trust. We thank Jennifer Hsiao (Harvard) for helpful discussions. RH, MK and NP were supported by the Yale SPORE in Skin Cancer, award number 1 P50 CA121974 (RH).

Author contributions

C.D.R.-E., N.D.R., F.P.L., L.B.A., N.P. and D.T.B. performed the analysis of the data. R.H. and M.K. provided biological data from the Yale Melanoma Genome Project. S.C. and R.C. performed the melanocyte experiments. C.D.R.-E., N.D.R., F.P.L., D.T.B. and D.J.A. wrote the paper and supervised the research.

Additional information

Supplementary Information accompanies this paper at <http://www.nature.com/naturecommunications>

Competing financial interests: The authors declare no competing financial interests.

Reprints and permission information is available online at <http://npg.nature.com/reprintsandpermissions/>

How to cite this article: Robles-Espinoza, C.D. *et al.* Germline MC1R status influences somatic mutation burden in melanoma. *Nat. Commun.* **7**:12064 doi: 10.1038/ncomms12064 (2016).



This work is licensed under a Creative Commons Attribution 4.0 International License. The images or other third party material in this article are included in the article's Creative Commons license, unless indicated otherwise in the credit line; if the material is not included under the Creative Commons license, users will need to obtain permission from the license holder to reproduce the material. To view a copy of this license, visit <http://creativecommons.org/licenses/by/4.0/>

© The Author(s) 2016